Defence Research and    Recherche et développement
Development Canada      pour la défense Canada

DEFENCE **R&D** DÉFENSE

# Micro-Doppler Analysis of Rotating Target in SAR

T. Thayaparan, S. Abrol and S. Qian

## Defence R&D Canada – Ottawa

Canada

# Micro-Doppler Analysis of Rotating Target in SAR

T. Thayaparan
Defence R&D Canada – Ottawa

S. Abrol
University of Ottawa

S. Qian
National Instruments

**Defence R&D Canada – Ottawa**

Technical Memorandum

DRDC Ottawa TM 2005-204

December 2005

# Abstract

Rotating targets cause phase modulation of the azimuthal phase history of a SAR system. The phase modulation may be seen as a time-dependent micro-Doppler (m-D) frequency. Due to their superior resolution potential, it is useful to analyze such signals with time-frequency analysis methods. This report presents two approches for extracting m-D features from SAR images. In order to extract m-D features from SAR images, the time domain radar return is decomposed in two separate ways. One is based on wavelet decomposition in which the returned signal is decomposed into a set of components that are represented at different wavelet scales. The components are then reconstructed by applying the inverse wavelet transform. This wavelet approach has been used in our previous m-D analysis work for a ISAR system, and it is presented here in the extraction of m-D features for a SAR system. The second approach is based on adaptive chirplet decompostion. This new approach is introduced as an alternative to the wavelet approach of decomposing the SAR radar return. The results from the wavelet and adaptive chirplet decompostion procedures are compared, and the chirplet-based approach establishes itself as a viable alternative. The chirplet based method of m-D extraction has been successfully applied to SAR data scene collected by the US Navy APY-6 radar. The rotating frequency of the antenna was calculated using this method and the results agree well with available ground truth data.

# Résumé

Les cibles rotatives causent la modulation de la phase azimutale d'un système SAR. La modulation de phase peut être considérée comme une fréquence micro-Doppler (m-D) variable dans le temps. Vu leur potentiel de résolution supérieure, il est utile d'analyser ces signaux au moyen de méthodes d'analyse temps-fréquence. Le présent rapport décrit deux méthodes d'extraction des caractéristiques m-D des images SAR. En vue d'extraire les caractéristiques m-D des images SAR, l'écho radar dans le domaine temps est décomposé de deux façons distinctes. L'une est basée sur la décomposition de l'ondelette dans laquelle l'écho est décomposé en un ensemble de composantes qui sont représentées sur différentes échelles d'ondelette. Les composantes sont ensuite reconstituées par l'application de la transformée d'ondelette inverse. Cette méthode à ondelette a été utilisée dans notre travail d'analyse m-D antérieur pour un système ISAR, et elle est présentée ici dans l'extraction des caractéristiques d'un système SAR. La seconde méthode est basée sur la décomposition de Chirplet adaptatif. Cette nouvelle méthode est introduite comme rechange de la méthode à ondelette pour décomposer l'écho du radar SAR. Les résultats des procédures de décomposition d'ondelette et de Chirplet adaptatif sont comparés, et la méthode basée sur Chirplet s'avère une méthode de rechange viable. La méthode basée sur Chirplet pour extraire les caractéristiques m D a été appliquée avec succès à la collecte de données de scène SAR au moyen du radar APY-6 de la marine américaine. La fréquence de rotation de l'antenne a été calculée au moyen de cette méthode, et les résultats concordent bien avec les données de réalité de terrain disponibles.

# Executive summary

SAR images are a high-resolution map of surface target areas and terrain in the range and cross-range dimension. If there are moving targets in the scene, SAR cannot simultaneously produce clear images of both these stationary targets and moving targets. Usually, moving targets appear as defocussed and spatially displaced objects superimposed on the SAR map. Moving targets affect the phase history of a SAR collection in a manner dependent on the particular motion of the target. Some targets contain parts that move relative to the target itself. Examples are rotating/vibrating parts such as wheels or engines. A special case is rotating point targets such as a rotating antenna. The resulting class of motions may aid target characterization and recognition. Rotations and vibrations can be observed by radar when the conditions are right. The phenomenon, as observed by radar, is termed micro-Doppler (m-D). In addition to the m-D, there may be a Doppler shift corresponding to the target body motion.

In this report, we examine the case of a rotating antenna on the ground. Such a rotating target causes sinusoidal phase modulation of the azimuth phase history of the SAR collection. The phase modulation may equivalently be seen as a time-varying Doppler frequency. Time-frequency methods are useful tools in the analysis of such signals as they use time integration while still allowing for non-stationary signals. Also, multicomponent signals may be analyzed. Therefore, a method for extracting target motion parameters is needed so that motion parameters may be estimated and targets can be identified.

This report presents two approches for extracting m-D features from SAR images. In order to extract m-D features from SAR images, the time domain radar return is decomposed in two separate ways. One is based on wavelet decomposition in which the returned signal is decomposed into a set of components that are represented at different wavelet scales. The components are then reconstructed by applying the inverse wavelet transform. This wavelet approach has been used in our previous m-D analysis work for a ISAR system, and it is presented here in the extraction of m-D features for a SAR system. The second approach is based on the adaptive chirplet decompostion. This new approach is introduced as an alternative to the wavelet approach of decomposing the SAR radar return. The results from the wavelet and adaptive chirplet decompostion procedures are compared, and the chirplet based approach establishes itself to be a viable alternative. The chirplet-based method of m-D extraction has been successfully applied to SAR data scene collected by the US Navy APY-6 radar. The rotating frequency of the antenna was calculated using this method and the results agree well with available ground truth. Such parameters may be useful for describing the target, or serve as inputs to automatic target recognition algorithms.

# Sommaire

Les images SAR sont une carte à haute résolution des aires de cibles de surface et du terrain sur le plan de la distance et de la largeur. Si la scène comprend des cibles mobiles, le SAR ne peut pas produire simultanément des images claires à la fois des cibles fixes et des cibles mobiles. D'habitude, les cibles mobiles se présentent sous la forme d'objets défocalisés et déplacés dans l'espace, superposés à la carte SAR. Les cibles mobiles influent sur la discordance de phase d'une collecte SAR d'une façon dépendant du mouvement particulier de la cible. Certaines cibles contiennent des parties qui se déplacent par rapport à la cible elle-même. Des exemples sont des parties rotatives ou vibratoires telles que les roues ou les moteurs. Un cas spécial est constitué par les cibles à point de rotation, comme les antennes rotatives. La classe de mouvements qui en résulte peut aider la caractérisation et la reconnaissance des cibles. Le radar permet d'observer les rotations et les vibrations lorsque les conditions sont appropriées. Ce phénomène, observé au radar, est appelé effet micro-Doppler (m-D). En plus de l'effet m-D, il peut y avoir un décalage Doppler correspondant au mouvement de l'objet cible.

Dans le présent rapport, nous examinons le cas d'une antenne rotative au sol. Une telle cible rotative cause la modulation sinusoïdale de la phase azimutale de la collecte SAR. La modulation de phase peut également être considérée comme une fréquence Doppler variable dans le temps. Les méthodes temps-fréquence sont des outils utiles pour analyser ces signaux, car elles font appel à l'intégration temporelle tout en admettant des signaux d'objets mobiles. De plus, elles permettent d'analyser des signaux à composantes multiples. Par conséquent, il faut une méthode pour extraire les paramètres de mouvement des cibles pour qu'on puisse estimer les valeurs des paramètres de mouvement et identifier les cibles.

Le présent rapport décrit deux méthodes d'extraction des caractéristiques m-D des images SAR. En vue d'extraire les caractéristiques m-D des images SAR, l'écho radar dans le domaine temps est décomposé de deux façons distinctes. L'une est basée sur la décomposition de l'ondelette dans laquelle l'écho est décomposé en un ensemble de composantes qui sont représentées sur différentes échelles d'ondelette. Les composantes sont ensuite reconstituées par l'application de la transformée d'ondelette inverse. Cette méthode à ondelette a été utilisée dans notre travail d'analyse m-D antérieur pour un système ISAR, et elle est présentée ici dans l'extraction des caractéristiques d'un système SAR. La seconde méthode est basée sur la décomposition d'un Chirplet adaptatif. Cette nouvelle méthode est introduite comme rechange de la méthode à ondelette pour décomposer l'écho du radar SAR. Les résultats des procédures de décomposition d'ondelette et de Chirplet adaptatif sont comparés, et la méthode basée sur Chirplet s'avère une méthode de rechange viable. La méthode basée sur Chirplet pour extraire les caractéristiques m D a été appli-

quée avec succès à la collecte de données de scène SAR au moyen du radar APY-6 de la marine américaine. La fréquence de rotation de l'antenne a été calculée au moyen de cette méthode, et les résultats concordent bien avec les données de réalité de terrain disponibles. Ces paramètres peuvent être utiles pour décrire la cible ou servir de valeurs d'entrée des algorithmes de reconnaissance automatique de cibles.

# Table of contents

This page intentionally left blank.

# 1  Introduction

## 1.1  Synthetic Aperture Radar

The concept of radar is actually quite simple. Microwave radiation is transmitted to a target location, and the reflected energy is received and measured by an antenna/receiver system. This idea, however simple, is applied in a tremendous variety of rather complex applications. One field of application is broad-area imaging. In such a system, the resolution is affected by the size of the aperture, (i.e., the area used to receive signals); a larger aperture results in a higher resolution. In other words, radar performance is inhibited by the size of the emitting antenna. A much larger antenna than can be practically employed is needed for an acceptable resolution. If the radar is equipped to a moving platform, such as a satellite or an aircraft, then it is possible to combine reflected signals from along the flight path to simulate (synthesize) a very long antenna. The radar transmits a wide beam of electromagnetic signals at a series of points along the flight path. Since the signals are coherent and always in phase, the radar return is collected and then combined in order to create high resolution images just as they would have been made if a very large antenna had been employed. In this way, a long aperture is artificially created. This is known as Synthetic Aperture Radar (SAR). Here, it is important to note that the radar is moving relative to the target. This is quite contrary to ISAR (Inverse Synthetic Aperture Radar) where an image is generated from reflected signals collected by a stationary radar from a moving target [1-7].

SAR systems usually produce two-dimensional images. One dimension is called the range and is obtained by precisely measuring the time from transmission of a signal to its return. The second dimension is known as the azimuth and is perpendicular to the range dimension. The azimuthal resolution is obtained by processing the Doppler phase of the radar return. What differentiates SAR from other radars is its ability to produce fine azimuth resolution [1-7].

SAR is a well established and useful technique of acquiring high-resolution images of an area of interest from airborne or space sensors [1-2]. A particular class of targets that pose a difficult challenge for target recognition is moving targets. If there are moving targets in the scene, SAR cannot simultaneously produce clear images of both of these stationary targets and moving targets [3-7]. Usually, moving targets appear as defocused and spatially displaced objects superimposed on the SAR map. Moving targets cause phase modulation of the azimuth phase history of a SAR collection. The phase modulation can be seen as a time-varying Doppler frequency. It is obvious that in some scenarios it is the moving objects that are of interest. Therefore, a method for extracting target motion parameters is needed so that motion parameters may be estimated and targets can be identified.

## 1.2 Micro-Doppler Phenomenon

When a radar transmits an electromagnetic signal to a target, the signal interacts with the target and then returns to the radar. Clearly, any changes in the properties of the returned signal are generally due to its interaction with the target. This being the case, the characteristics of the target in question are reflected in the returned signal, and it follows that various properties of the relevant target can be extracted from the returned signal. For example, when the target is moving, the carrier frequency of the returned signal will be shifted due to the Doppler effect. This Doppler frequency shift can then be used to determine the radial velocity of the moving target.

It frequently occurs that a target or some structure on the target is vibrating or rotating in addition to the target's translation. These vibrations and rotations are referred to as micro-motion dynamics. The micro-motion dynamics of a target generate frequency modulations on the returned signal in addition to the Doppler frequency shift caused by the target's translational motion. In fact, the frequency modulations on the returned signal induced by the micro-motions produce sidebands about the target's Doppler frequency. The frequency modulation due to micro-motion dynamics is called the micro-Doppler (m-D) phenomenon [7-13].

While the Doppler frequency shift created by the translational motion of the target is time-invariant at a constant velocity, the Doppler frequency shift generated by micro-motion dynamics is a time-varying function that imposes a periodic time-varying modulation onto the carrier frequency. The modulation contains harmonic frequencies that depend on the carrier frequency, the vibration or rotation rate, and the angle between the direction of vibration and the direction of the radar's incident wave.

The m-D phenomenon is of interest because information regarding a target's micro-motion dynamics is preserved in the returned radar signal. The m-D phenomenon is commonly encountered in radar returned signals because real world targets (e.g., helicopter, vehicle, rotating antenna) are usually engaged in complicated maneuvers that incorporate translation, vibrational and rotational motions. The mechanical vibration/rotation of a target or part of the target's structure appears in a radar image as smeared features across the cross-range dimension of the image and induces frequency modulation on radar returned signals [7-17]. On the other hand, m-D features could provide distinctive information for recognition of targets of interest. They have been used to identify the natural resonant frequency of a tractor-trailer truck [14]. The m-D features of a Jet Engine Modulation (JEM) lines in a Mi-24 Hind-D helicopter are also used to estimate the turbine rotation rate and the number of turbine blades [15]. Also, research has been conducted on radar Doppler signatures in the area of human gait analysis [7,9,11,13, 18-19].

It is reasonable to expect that the m-D features representing the micro-motions of a target can be extracted from the returned signal, much in the same way as properties are extracted from radar returns of targets undergoing only translational motion. Since different targets produce different micro-motions, every target would have its own "m-D signature", making it possible to distinguish and identify targets under consideration based on the additional information provided by the m-D features. Hence, an effective method is needed for extracting m-D features in order to fully exploit the additional and unique information they provide [11].

In this work, we extract the m-D features relating to a rotating antenna in a SAR target scenarios. The m-D for such rotating target may be seen as a sinusoidal phase modulation of the SAR azimuth phase history. Along with the wavelet decomposition method used in previous works of m-D analysis [11-13], we introduce an adaptive chirplet decomposition method to extract m-D features. The goal of this report is to find a method of extracting m-D features in SAR and detect useful targets. These m-D features may provide additional information for target recognition complementary to existing recognition methods.

# 2 Method of Micro-Doppler Feature Extraction

Joint time-frequency analysis is the base of most of the existing methods used to extract m-D features [7-13]. The procedure of wavelet analysis incorporated with time-frequency analysis (specifically, the short-time Fourier transform) has been applied in our previous works for a ISAR system [11-13]. Here, the approach is used in a SAR target scenarios. Also, we introduce a new procedure for m-D analysis, namely, the adaptive chirplet decomposition incorporated with the time-frequency distribution series.

## 2.1 Wavelet Analysis

A very useful tool in many recent signal processing applications such as detecting the discontinuity of a signal, de-noising a signal, and image compression, the wavelet transform results in an efficient representation of highly non-stationary signals [20-24]. The main motivation for applying wavelet analysis in the extraction of m-D features is that the micro-motion dynamics of a target that induce m-D features change at a rate much faster than the target body itself. Wavelet analysis has the capability of detecting rapid changes of a signal [20-24]. Therefore, wavelet analysis seems ideal for the extraction of m-D features and the wavelet transform can be considered a powerful tool for the task.

The wavelet analysis is actually quite complex and contains a large number of steps. The wavelet transform is applied by using a tree of digital filter banks based upon the multi-resolution analysis theory [20-24]. In order to effectively extract m-D features from the returned signal, a four level decomposition tree is utilized to represent the returned radar signal. Using the wavelet transform, the signal is first broken down into its constituent parts consisting of the four detail levels containing the m-D features and the left over stationary approximation representing the body vibration. The inverse wavelet transform is then used to reconstruct the decomposed wavelet components. During the reconstruction process of the detail levels, only the wavelet coefficients that are related to the m-D features of the signal are used while the other coefficients are set to zero. The same process is also used in the reconstruction of the stationary part of the target's body. The result of the wavelet analysis is the separation of the target's micro-motion dynamics and the extraction of the m-D features. This method has been tested previously and shown to be successful with other data sets [11-15].

The tree of digital filter banks for computing the discrete wavelet transform is given in Figure 1 (this is a four level decomposition tree). *L* and *H* represent pairs of
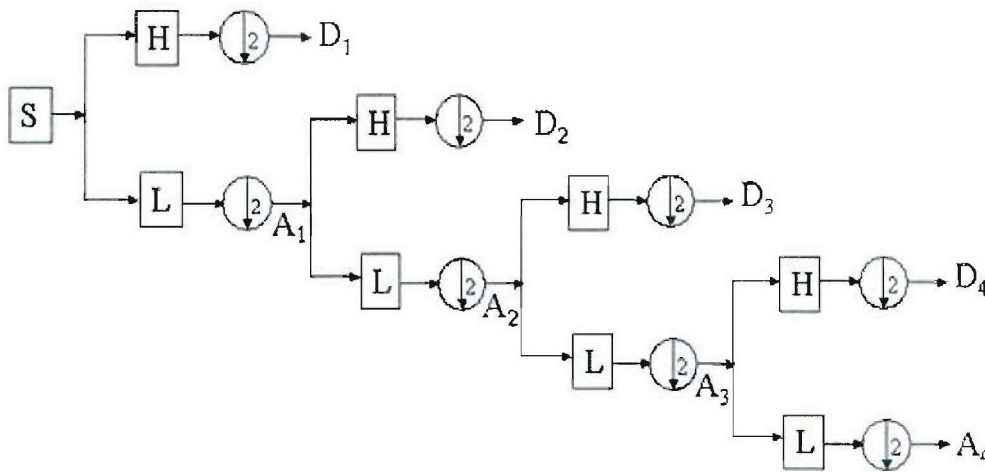
**Figure 1:** *The tree of filter banks for computing the discrete wavelet transform.*

discrete low-pass and high-pass filters. As demonstrated in this figure, the original signal $S$ is decomposed into its constituent parts consisting of $D_1$, $D_2$, $D_3$, $D_4$, and $A_4$. In other words, after decomposition $S = A_4 + D_1 + D_2 + D_3 + D_4$. Now, the wavelet transform has decomposed the signal into five parts; the four detail levels and the stationary approximation. Generally, these decomposed parts, by themselves, do not represent motion dynamics of the target in question. Depending on the physical quantity that one wishes to estimate, the decomposed parts of the signal may need to be combined in various ways in order to represent the m-D features for which motion parameters are required.

## 2.2   Adaptive Chirplet Analysis

Here, an alternative to wavelet analysis, the so-called adaptive chirplet analysis, is proposed in the extraction of m-D features from a radar return. A chirplet is a windowed portion of a chirp. A chirp being a function very similar to a harmonic function but instead of having a fixed period, the period changes with time along the function. The chirplet is to a wavelet as the chirp is to a wave, as shown in Figure 2. Many events, especially those found in nature, can be modelled as the superposition of short-lived chirp functions. The chirplet transform has been recently used in areas such as multi-component signal detection, instantaneous frequency estimation, time-varying filter design, and interference excision [9, 20, 25].

In this work, the adaptive Gaussian chirplet decomposition is employed to extract
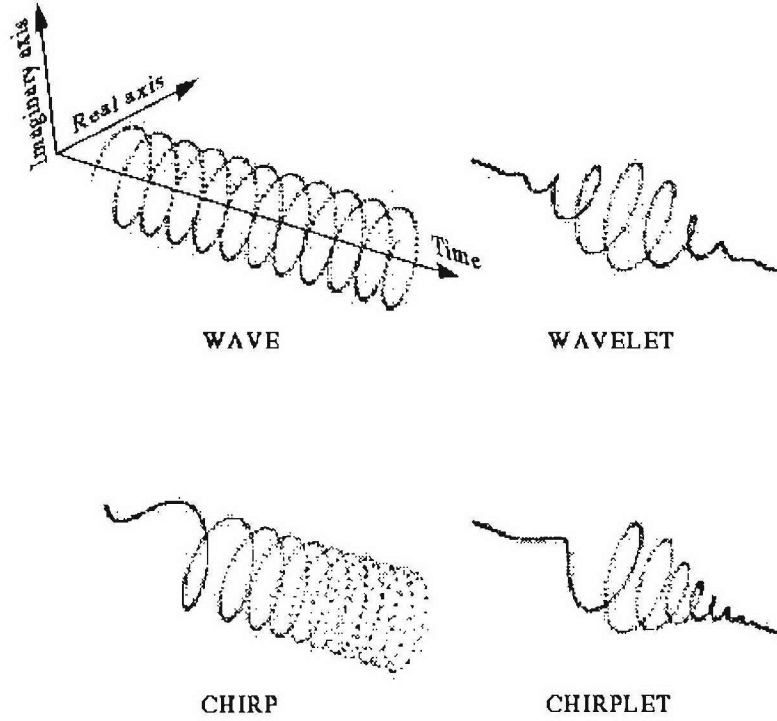
**Figure 2:** *Chiplet versus Wavelet*

m-D features. The Gaussian chirplet is defined as [20,25]

$$h_k(t) = \sqrt[4]{\tfrac{\alpha_k}{\pi}} \exp\left\{ -\tfrac{\alpha_k}{2}(t-t_k)^2 + j\left(\omega_k(t-t_k) + \tfrac{\beta_k}{2}(t-t_k)^2\right)\right\}$$
$$\alpha_k > 0 \tag{1}$$
$$t_k, \omega_k, \beta_k \in R$$

where $(t_k, \omega_k)$ indicates the time and frequency center of the linear chirp function, the variance $\alpha_k$ controls the width of the chirp function, and the parameter $\beta_k$ determines the rate of change of frequency. When the chirp rate $\beta_k$ is equal to zero and the parameter $\alpha_k$ approaches zero, the linear chirplet function $h_k(t)$ reduces to a sinusoidal signal.

The adaptive spectrogram for the Gaussian chirplet is given as [20]

$$AS(t,\omega) = 2\sum_k |B_k|^2 \exp\left\{ -\alpha_k(t-t_k)^2 - \frac{1}{\alpha_k}(\omega - \omega_k - \beta_k t)^2 \right\} \tag{2}$$

The algorithm used here estimates the optimal elementary functions in the adaptive signal decomposition. Converting the optimization process to a traditional curve-fitting problem is the basic idea behind this algorithm. The relationship between

DRDC Ottawa TM 2005-204

the estimated parameters and testing variables is given by the function

$$P\left(\alpha_k, t_k, \omega_k, \beta_k; \alpha_{k,m}, t_{k,m}, \omega_{k,m}, \beta_{k,m}\right) \qquad (3)$$

as follows

$$
\begin{aligned}
&P\left(\alpha_k, t_k, \omega_k, \beta_k; \alpha_{k,m}, t_{k,m}, \omega_{k,m}, \beta_{k,m}\right) \\
&= \frac{|A_k|}{\sqrt[4]{\left(\dfrac{1}{4\alpha_{k,m}\alpha_k}\right)\left[\left(\alpha_k+\alpha_{k,m}\right)^2+\left(\beta_k-\beta_{k,m}\right)^2\right]}} \\
&\times \exp\left\{\frac{\alpha_{k,m}^2\alpha_k+\alpha_{k,m}\alpha_k^2+\alpha_{k,m}\beta_k^2+\alpha_k\beta_{k,m}^2}{2\left[\left(\alpha_k+\alpha_{k,m}\right)^2+\left(\beta_k-\beta_{k,m}\right)^2\right]}\left(t_k-t_{k,m}\right)^2\right\} \\
&\times \exp\left\{\frac{\alpha_{k,m}\beta_k+\alpha_k\beta_{k,m}}{\left(\alpha_k+\alpha_{k,m}\right)^2+\left(\beta_k-\beta_{k,m}\right)^2}\left(t_k-t_{k,m}\right)\left(\omega_k-\omega_{k,m}\right)\right\} \\
&\times \exp\left\{\frac{\alpha_k+\alpha_{k,m}}{2\left[\left(\alpha_k+\alpha_{k,m}\right)^2+\left(\beta_k-\beta_{k,m}\right)^2\right]}\left(\omega_k-\omega_{k,m}\right)^2\right\}
\end{aligned}
\qquad (4)
$$

This can be written as

$$
\begin{aligned}
&P\left(\alpha_k, t_k, \omega_k, \beta_k; \alpha_{k,0}, t_{k,n}, \omega_{k,m}, \beta_{k,0}\right) \\
&= \left|\left\langle s_k, h_{\alpha_{k,0}, t_{k,n}, \omega_{k,m}, \beta_{k,0}}\right\rangle\right| \\
&= a\left(t_{k,n}\right) e^{-b\left[\varpi\left(t_{k,n}\right)-\omega_{k,m}\right]^2}
\end{aligned}
$$

where

$$a\left(t_{k,n}\right) = \frac{|A_k|}{\sqrt[4]{\left(\dfrac{1}{4\alpha_{k,0}\alpha_k}\right)\left[\left(\alpha_k+\alpha_{k,0}\right)^2+\left(\beta_k-\beta_{k,0}\right)^2\right]}} \exp\left\{\frac{\left(t_k-t_{k,n}\right)^2}{2\left(\alpha_k^{-1}+\alpha_{k,0}^{-1}\right)}\right\} \qquad (5)$$

$$\varpi\left(t_{k,n}\right) = \omega_k - \frac{\alpha_{k,0}\beta_k+\alpha_k\beta_{k,0}}{\alpha_k+\alpha_{k,0}}\left(t_k-t_{k,n}\right)$$

and

$$b = \frac{\alpha_k+\alpha_{k,0}}{2\left[\left(\alpha_k+\alpha_{k,0}\right)^2+\left(\beta_k-\beta_{k,0}\right)^2\right]}$$

Since both sides of the previous equation are greater than zero, we have

$$
\begin{aligned}
&\ln\frac{\left|\left\langle s_k, h_{\alpha_{k,0}, t_{k,n}, \omega_{k,i}, \beta_{k,0}}\right\rangle\right|}{\left|\left\langle s_k, h_{\alpha_{k,0}, t_{k,n}, \omega_{k,j}, \beta_{k,0}}\right\rangle\right|} \\
&= b\left[\left(\varpi\left(t_{k,n}\right)-\omega_{k,j}\right)^2-\left(\varpi\left(t_{k,n}\right)-\omega_{k,i}\right)^2\right] \\
&= 2b\varpi\left(t_{k,n}\right)\left(\omega_{k,i}-\omega_{k,j}\right)-b\left(\omega_{k,i}^2-\omega_{k,j}^2\right)
\end{aligned}
\qquad (6)
$$

The following three test points are inserted into equation 5.

$$\begin{pmatrix} \alpha_{k,0}, t_{k,0}, \omega_{k,-1}, \beta_{k,0} \\ \alpha_{k,0}, t_{k,0}, \omega_{k,0}, \beta_{k,0} \\ \alpha_{k,0}, t_{k,0}, \omega_{k,1}, \beta_{k,0} \end{pmatrix} \tag{7}$$

This results in the linear system given below

$$\left[ \frac{(\omega_{k,0} - \omega_{k,-1})(\omega_{k,-1}^2 - \omega_{k,0}^2)}{(\omega_{k,0} - \omega_{k,1})(\omega_{k,1}^2 - \omega_{k,0}^2)} \right] \left[ \begin{array}{c} x_\omega \\ b \end{array} \right] = \left[ \begin{array}{c} \ln \frac{|\langle s_k, h_{\alpha_{k,0},t_{k,0},\omega_{k,0},\beta_{k,0}} \rangle|}{|\langle s_k, h_{\alpha_{k,0},t_{k,0},\omega_{k,-1},\beta_{k,0}} \rangle|} \\ \ln \frac{|\langle s_k, h_{\alpha_{k,0},t_{k,0},\omega_{k,0},\beta_{k,0}} \rangle|}{|\langle s_k, h_{\alpha_{k,0},t_{k,0},\omega_{k,1},\beta_{k,0}} \rangle|} \end{array} \right] \tag{8}$$

where

$$x_\omega = 2b\varpi(t_{k,0})$$
$$b > 0$$
$$\varpi(t_{k,0}) \in R$$

After $b$ and $\varpi(t_{k,0})$ are found from the above system, $a(t_{k,0})$ is computed using equation 4.

$$\ln a(t_{k,0}) = \ln |\langle s_k, h_{\alpha_{k,0},t_{k,n},\omega_{k,m},\beta_{k,0}} \rangle| + b(\varpi(t_{k,0}) - \omega_{k,m})^2 \tag{9}$$

Similarly, by applying the test points

$$\begin{pmatrix} \alpha_{k,0}, t_{k,1}, \omega_{k,-1}, \beta_{k,0} \\ \alpha_{k,0}, t_{k,1}, \omega_{k,0}, \beta_{k,0} \\ \alpha_{k,0}, t_{k,1}, \omega_{k,1}, \beta_{k,0} \end{pmatrix} \tag{10}$$

another set of intermediate variables $\varpi(t_{k,1})$ and $a(t_{k,n})$ are obtained. Letting

$$r = \frac{\alpha_{k,0}\beta_k + \alpha_k\beta_{k,0}}{\alpha_k + \alpha_{k,0}} \tag{11}$$

and substituting into equation 4 gives

$$\varpi(t_{k,n}) = \omega_k - r(t_k - t_{k,n}) \tag{12}$$

Using $\varpi\left(t_{k,0}\right)$ and $\varpi\left(t_{k,1}\right)$, the variable $r$ can be computed.

$$r = \frac{\varpi\left(t_{k,0}\right) - \varpi\left(t_{k,1}\right)}{t_{k,0} - t_{k,1}} \tag{13}$$

Now, the parameters $\alpha_k$ and $\beta_k$ can be determined from the following

$$\left\{\begin{array}{l} b = \frac{\alpha_k + \alpha_{k,0}}{2\left[\left(\alpha_k + \alpha_{k,0}\right)^2 + \left(\beta_k - \beta_{k,0}\right)^2\right]} \\ r = \frac{\alpha_k \beta_{k,0} + \alpha_{k,0}\beta_k}{\alpha_k + \alpha_{k,0}} \end{array}\right. \tag{14}$$

Using mathematical manipulations, the following is obtained.

$$\left\{2b\left[\left(\frac{\alpha_{k,0}}{r - \beta_{k,0}}\right)^2 + 1\right]\left(\beta_k - \beta_{k,0}\right) - \frac{\alpha_{k,0}}{r - \beta_{k,0}}\right\}\left(\beta_k - \beta_{k,0}\right) = 0 \tag{15}$$

The solution to the above equation is given by

$$\beta_k = \left\{\begin{array}{l} \beta_{k,0} + \frac{\alpha_{k,0}}{2b\left(r - \beta_{k,0}\right)\left[\left(\frac{\alpha_{k,0}}{r - \beta_{k,0}}\right)^2 + 1\right]} \\ \\ \beta_{k,0} \end{array}\right. \tag{16}$$

If $\beta_k = \beta_{k,0}$, then from equation 10.62 one gets

$$r = \beta_{k,0} \tag{17}$$

and

$$\alpha_k = \frac{1}{2b} - \alpha_{k,0} \tag{18}$$

Otherwise,

$$\begin{array}{l} \alpha_k = \frac{\beta_k - r}{r - \beta_{k,0}}\alpha_{k,0} \\ \alpha_k > 0 \end{array} \tag{19}$$

Now that $\alpha_k$ and $\beta_k$ are known, the time parameter $t_k$ can be computed from 10.53 as follows.

$$t_k = \frac{\alpha_k^{-1} + \alpha_{k,0}^{-1}}{t_{k,0} - t_{k,1}} \ln \frac{a\left(t_{k,0}\right)}{a\left(t_{k,1}\right)} - \frac{t_{k,0} + t_{k,1}}{2} \tag{20}$$

Finally, the frequency parameter $\omega_k$ can be solved from 10.63

$$\omega_k = \varpi\left(t_{k,0}\right) + r\left(t_k - t_{k.0}\right) \tag{21}$$

Recent studies show that radar signal can be properly modeled using the chirplet basis function. Many natural phenomena, for instance, signals encountered in radar systems [26-28], the impulsive signal that is dispersed by the ionosphere [29], and seismic signals [30], are modeled as chirplet type functions. The chirplet function has many striking characteristics. 1) The chirplet basis is a well understood four-parameter function, $\alpha_k, \beta_k, t_k,$ and $\omega_k$, localized in the joint time-frequency plane. Only a moderate computation time is needed to search for the basis parameters. 1) Since both the amplitude modulation (AM) and frequency modulation (FM) are part of the basis function, the chirplet can more efficiently represent the reflected signal from a target with a rotating part. Only a few set of these bases are needed to approximate the time-frequency structure of the radar signal. 3) More importantly, the radar returns from the target body and the rotating part can be more easily separated based on the parameters of the chirplet bases, particularly $\alpha_k$ and $\beta_k$. This is because signals from the main body and the rotating part are captured by chirplet bases with different parameters. We separate the body signal from the rotating part using threshold values of $\alpha_k$ and $\beta_k$. After the separation, we process the main body signal and the rotating part signal individually for better information extraction. This includes both the extraction of the geometrical features from the main body and the m-D features from the moving parts.

Following the extraction of m-D features from the radar returned signal using either wavelet or chirplet analysis, the time-frequency signatures of the m-D features can be utilized to visualize the oscillation and to extract motion parameters related to the target of interest. The reason for this is that the joint time-frequency analysis can provide time-varying Doppler frequency information. From the joint time-frequency representation of the m-D features, the motion parameters of a target such as the period and amplitude of the oscillation can be estimated [11-13].

To further the analysis of the extracted m-D features, the autocorrelation of the m-D time sequence signals can be computed and investigated. The autocorrelation of time sequence signals has already been used by Bell and Grubbs to es-

timate the vibration/rotation rate of micro-motions from a signal containing both vibrational/rotational and stationary parts [31]. It is probable that the estimated rate will be more accurate if this approach is used on data including only vibrational/rotational components obtained from the wavelet decomposition. This is because the return from the stationary parts strongly overlaps with the return from the vibrational/rotational parts in the Doppler frequency spectrum. Namely, signals from stationary parts and rotating parts superimpose on each other and thus are separable. The extracted m-D features are employed to estimate the target's motion parameters.

# 3 Micro-Doppler Analysis

The sample data sets are APY-6 collected at PAX for a rotating antenna. The parameters of the SAR system used to collect this set of data are shown in Table 1. The data has been pulse compressed and motion compensated to the first level. This is an initial data distribution and there may be undiscovered flaws in the processing. A Hamming window is applied to suppress range side-lobes. One thousand twenty four samples were processed. However, the data cuts may not contain edge samples that are reduced by the IF filter. Full data cuts are 72 seconds long and there are 2048 pulses, 1024 range bins and 8 bytes per complex sample. Using this data set and employing the proposed method, the rotation rate of the antenna is estimated. The rotation rate of the rotating antenna is known to be 4.7 seconds.

The original SAR image is shown in Figure 3. The Doppler smearing due to the rotating parts is often well localized in a finite number of range cells. It is reasonable to process the Doppler signal for each range cell independently. Since the ground truth of the target is already known, the data between the range cells 121 and 125 was analyzed using the wavelet decomposition method and the adaptive chirplet decomposition method. Therefore, the discussion of this report will deal exclusively with these range cells. Figure 4 shows the zoomed in SAR image between the range cells 115 and 130.

The following two subsections give the results obtained after signal analysis and processing using both the wavelet decomposition method and the adaptive chirplet decomposition method for range cells 123 and 124.

## 3.1 Wavelet Analysis

The analysis of the Doppler signals using the wavelet decomposition method is given in Figures 5 through 18 for range cells 123 and 124. The analysis of each range cell includes:

1. Time-series of the original signal,

2. Fourier transform of the original signal,

*Table 1: The characteristics of SAR*

| Center frequency | 9.65 GHz |
|---|---|
| Pulse repetition Interval (PRI) | 1/1200 seconds |
| Bandwidth | 150 MHz |
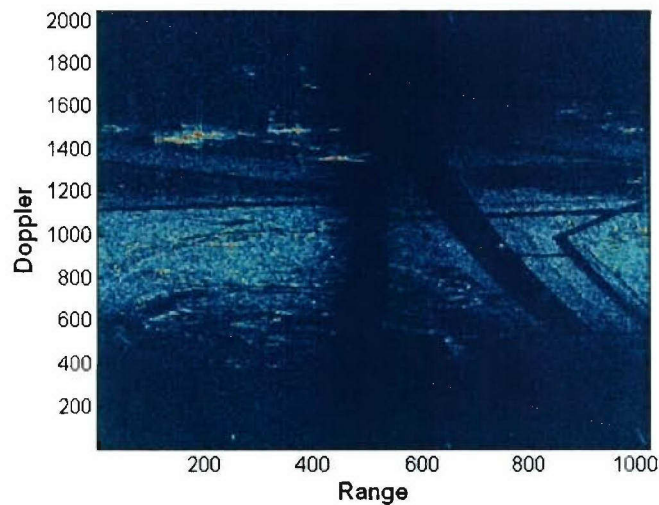
*Figure 3: The original SAR image.*

3. Time-frequency signature of the original signal,

4. Time-frequency signature of the extracted body signal,

5. Time-frequency signature of the extracted oscillating signal,

6. Autocorrelation function versus time for the extracted body signal, and

7. Autocorrelation function versus time for the extracted oscillating signal.

The wavelet transform method consists of decomposing the original signal into components and recombining these components in various groupings in order to obtain the reconstructed signals that represent the desired features. In this case, the features extracted are the body signal and the oscillating signal.
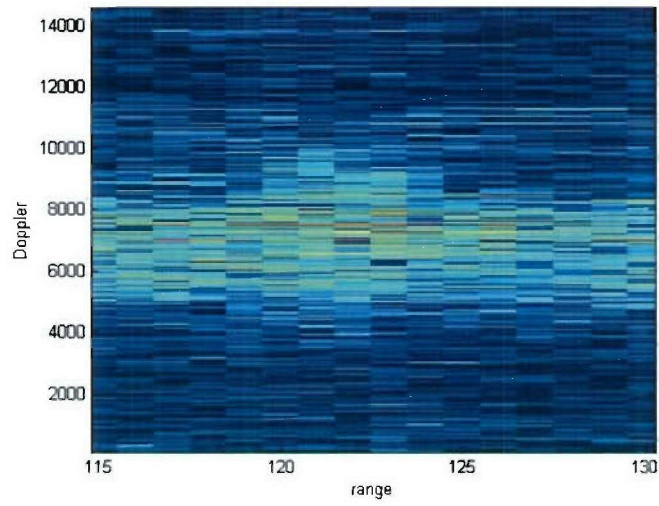
**Figure 4:** *The zoomed in SAR image.*
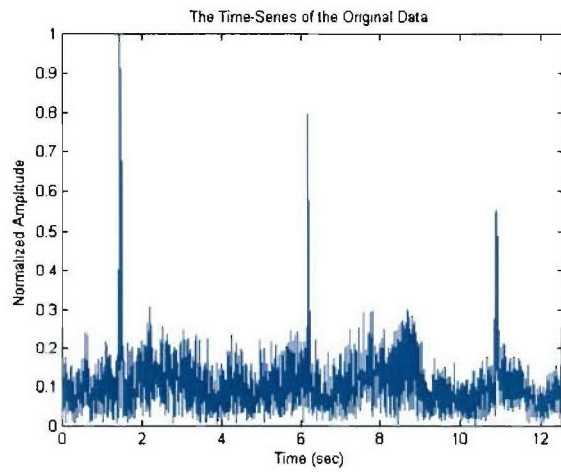
**Figure 5:** *Time-series of the original signal at range cell 123*
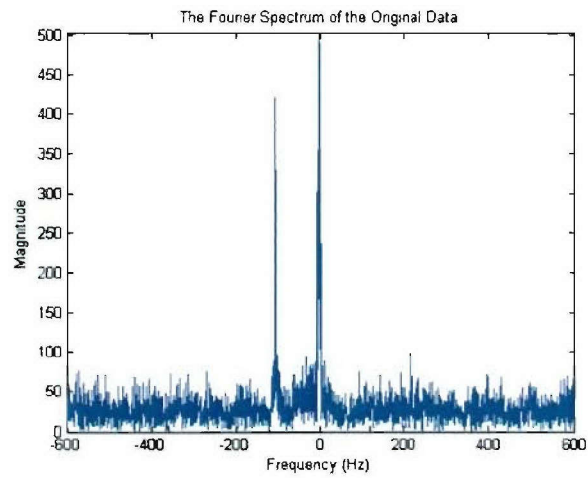


**Figure 6:** *Fourier transform of the original signal at range cell 123*

**Spectrum**

**TF Signature of the Original Signal**
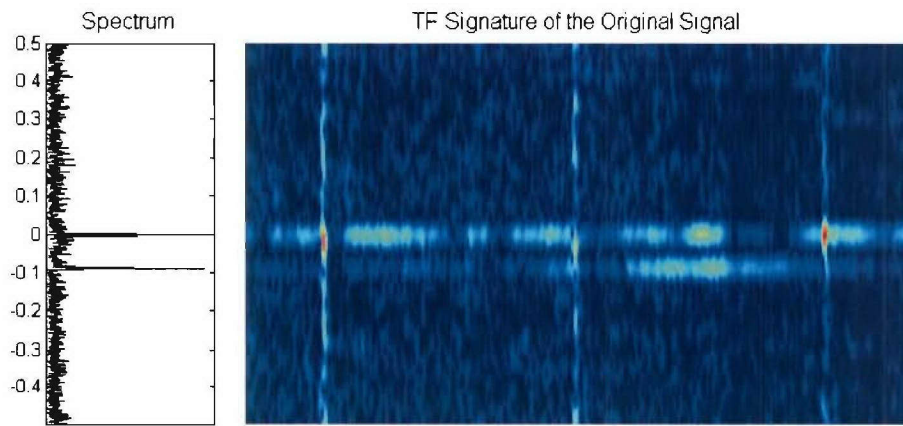
*Figure 7: Time-frequency signature of the original signal at range cell 123*
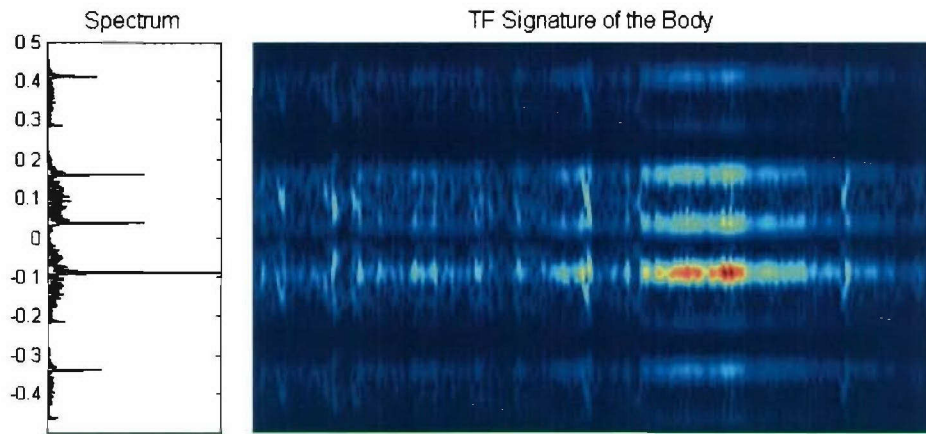
**Figure 8:** *Time-frequency signature of the extracted body signal at range cell 123*
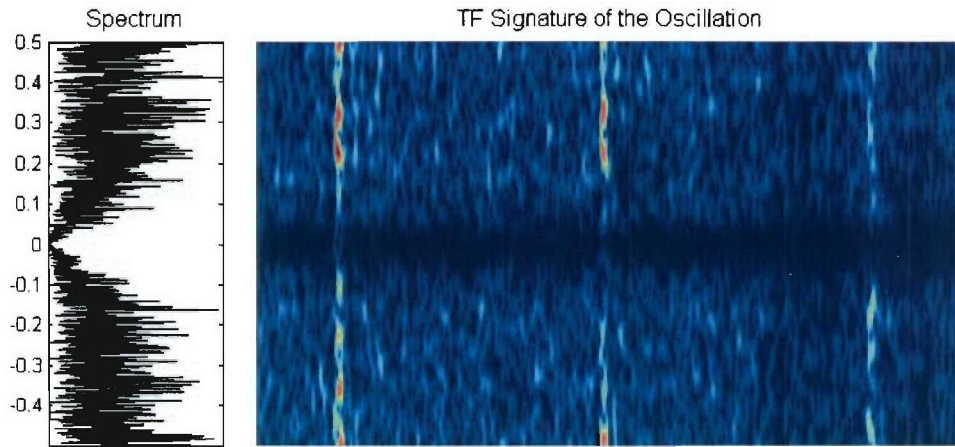
**Figure 9:** *Time-frequency signature of the extracted oscillating signal at range cell 123*
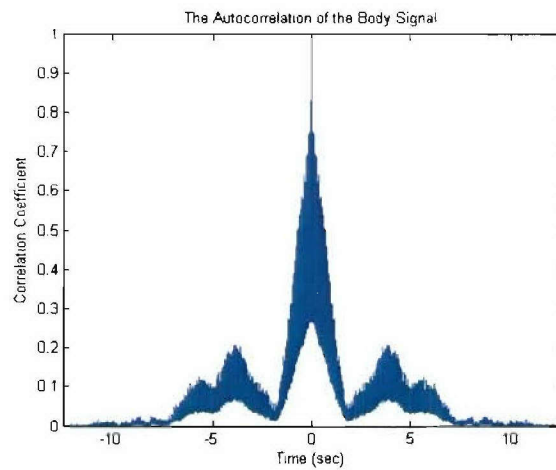


**Figure 10:** *Autocorrelation function versus time for the extracted body signal at range cell 123*
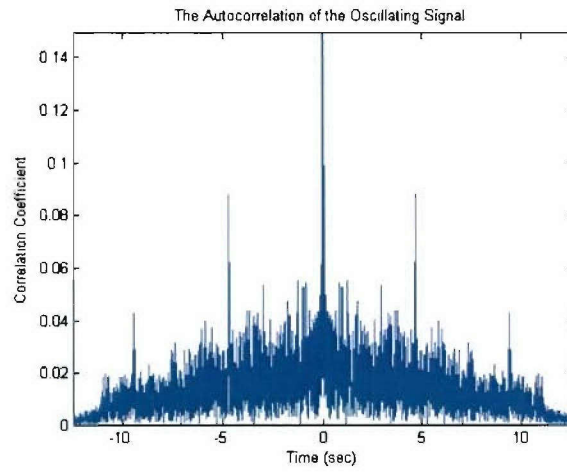
**Figure 11:** *Autocorrelation function versus time for the extracted oscillating signal at range cell 123*
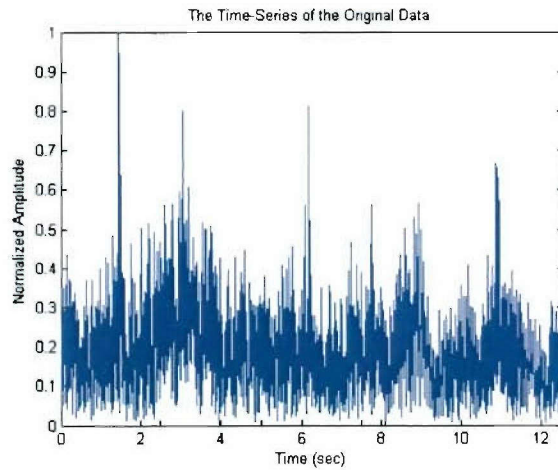


**Figure 12:** *Time-series of the original signal at range cell 124*
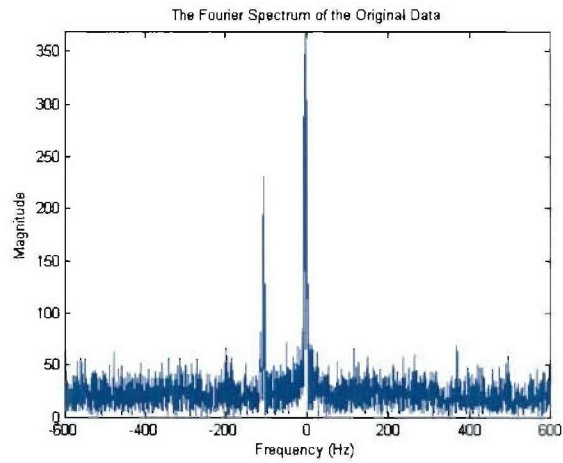
*Figure 13: Fourier transform of the original signal at range cell 124*
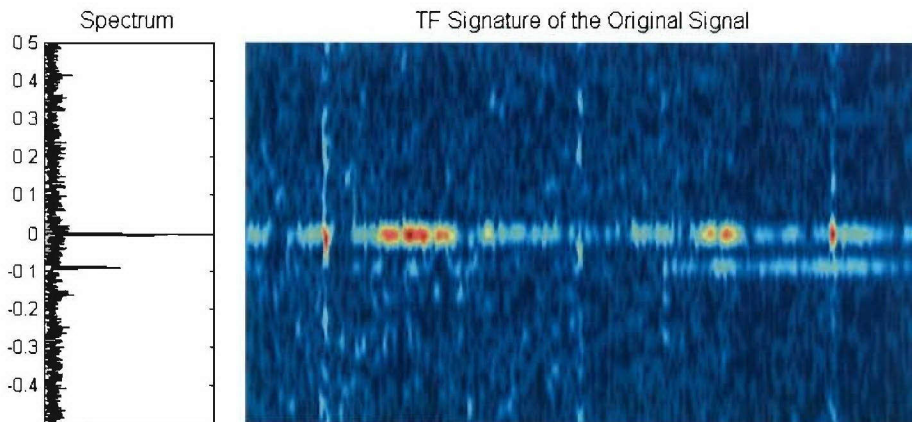


*Figure 14: Time-frequency signature of the original signal at range cell 124*
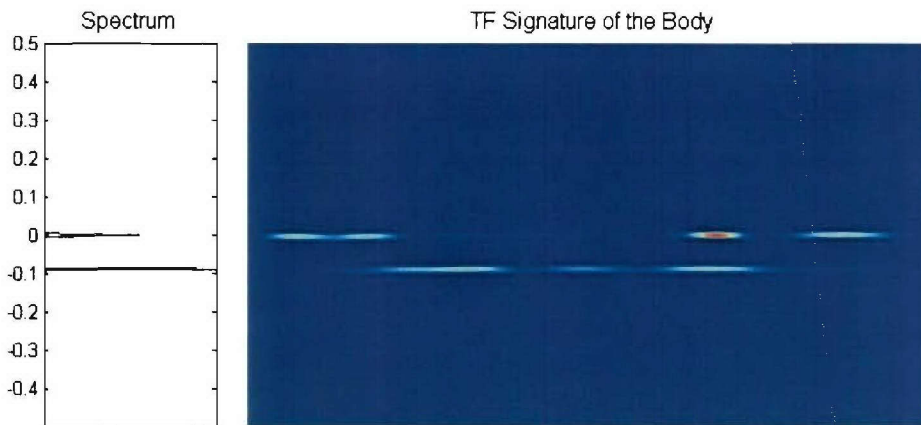
***Figure 15:*** *Time-frequency signature of the extracted body signal at range cell 124*
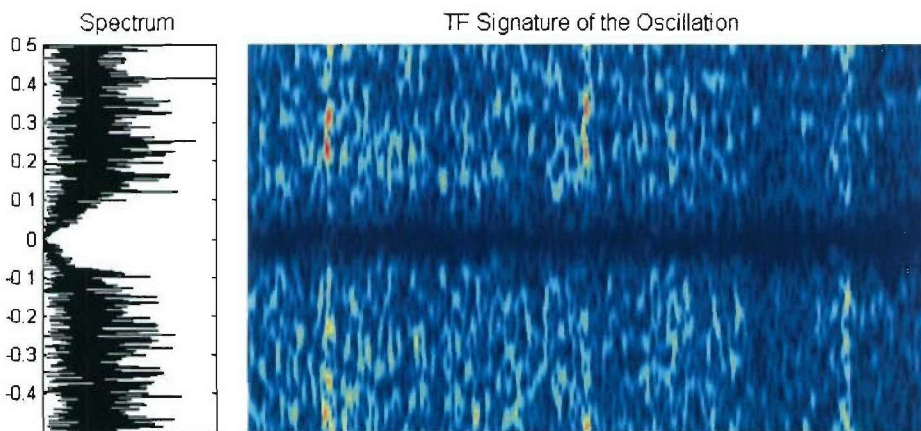


***Figure 16:*** *Time-frequency signature of the extracted oscillating signal at range cell 124*
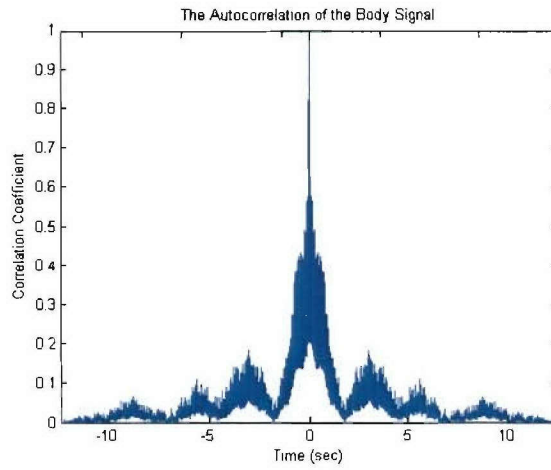
**Figure 17:** *Autocorrelation function versus time for the extracted body signal at range cell 124*
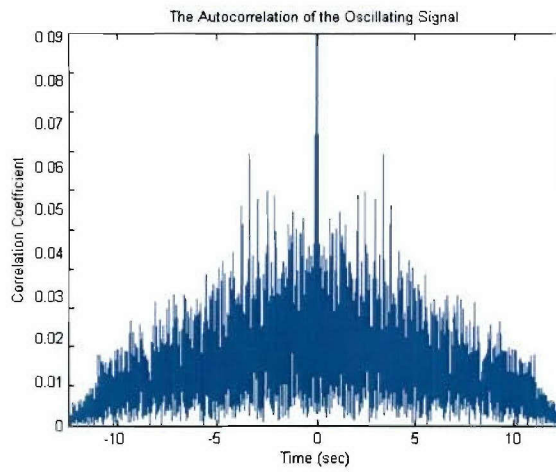


**Figure 18:** *Autocorrelation function versus time for the extracted oscillating signal at range cell 124*

## 3.2 Adaptive Chirplet Analysis

The analysis of the Doppler signals using the adaptive chirplet decomposition is given in Figures 19 through 32 for range cells 123 and 124. Similar to wavelet analysis, the analysis of each range cell includes:

1. Time-series of the original signal,

2. Fourier transform of the original signal,

3. Time-frequency signature of the original signal,

4. Time-frequency signature of the extracted body signal,

5. Time-frequency signature of the extracted oscillating signal,

6. Autocorrelation function versus time for the extracted body signal, and

7. Autocorrelation function versus time for the extracted oscillating signal.

As with the wavelet transform method, the features extracted here are the body signal and the oscillating signal.
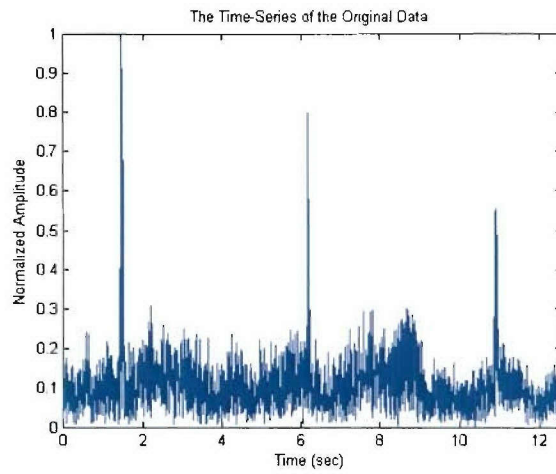
*Figure 19:* Time-series of the original signal at range cell 123
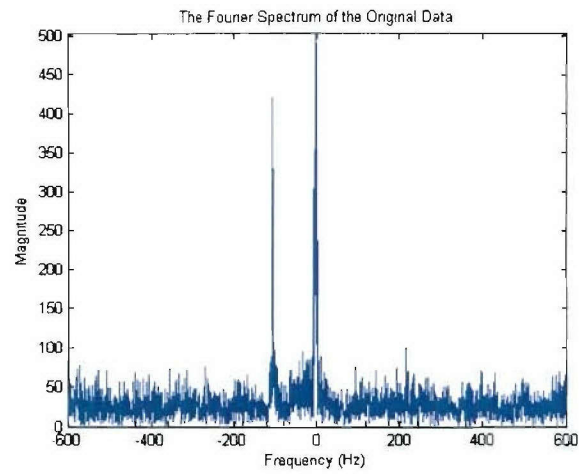


*Figure 20:* Fourier transform of the original signal at range cell 123
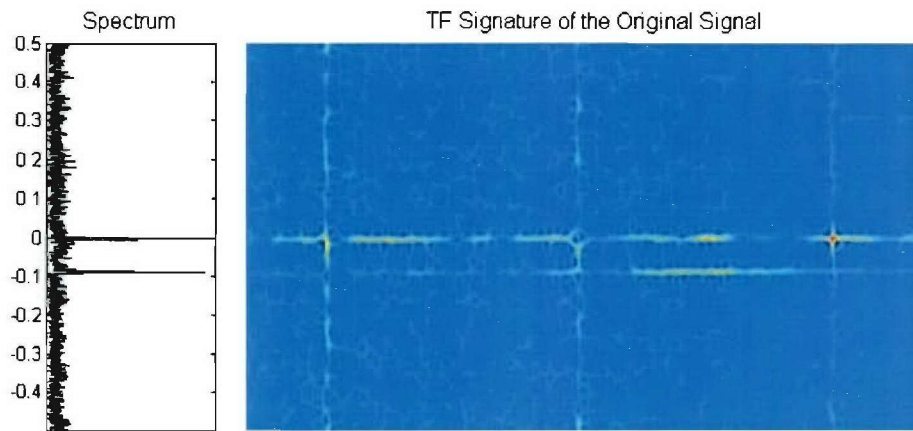
**Figure 21:** *Time-frequency signature of the original signal at range cell 123*
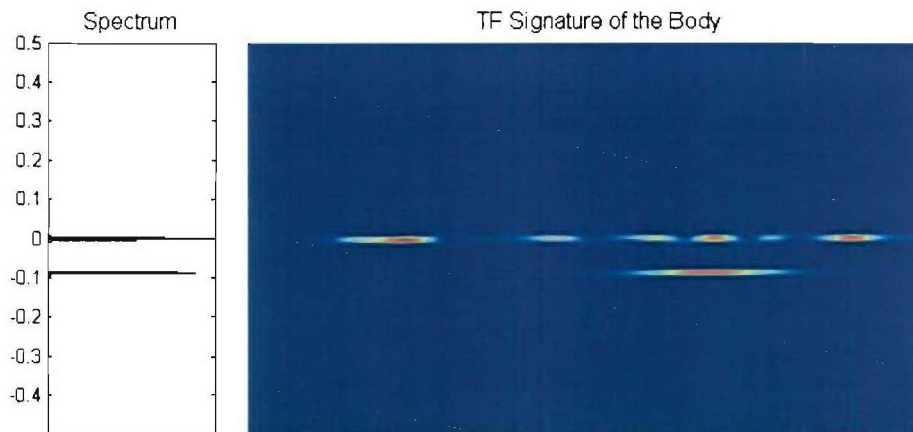


**Figure 22:** *Time-frequency signature of the extracted body signal at range cell 123*
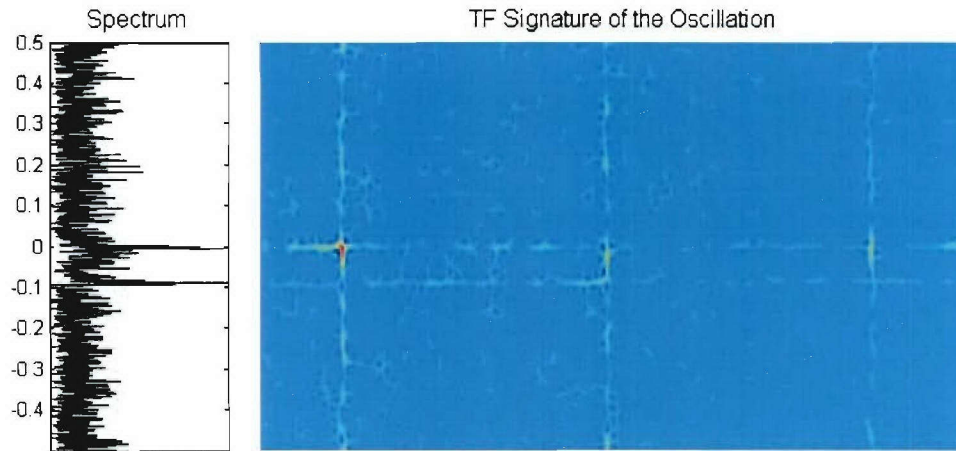
**Figure 23:** *Time-frequency signature of the extracted oscillating signal at range cell 123*
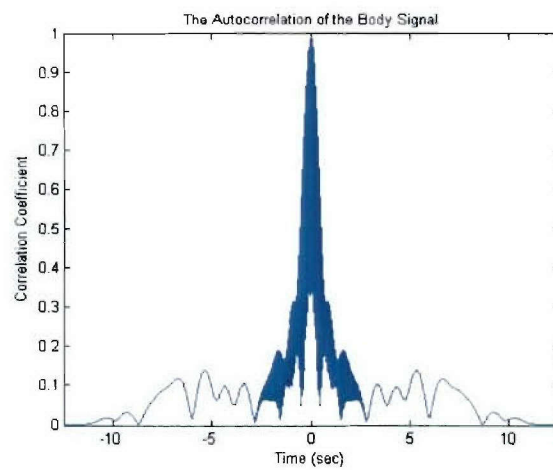


**Figure 24:** *Autocorrelation function versus time for the extracted body signal at range cell 123*
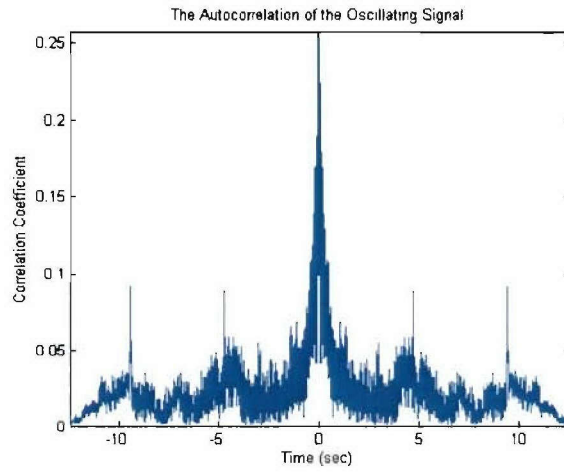
*Figure 25: Autocorrelation function versus time for the extracted oscillating signal at range cell 123*
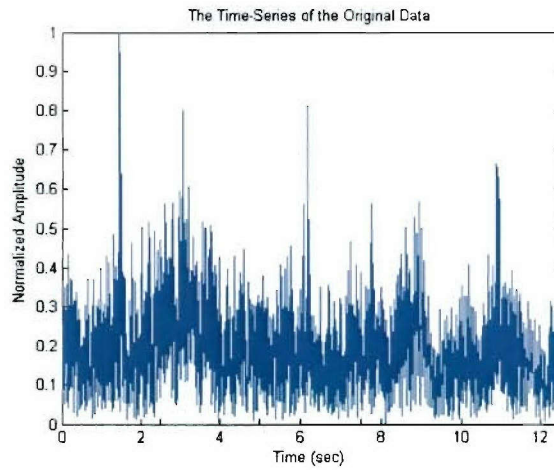


*Figure 26: Time-series of the original signal at range cell 124*
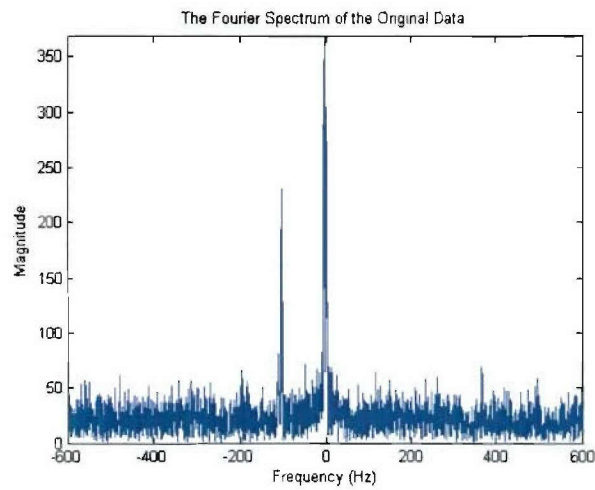
*Figure 27: Fourier transform of the original signal at range cell 124*
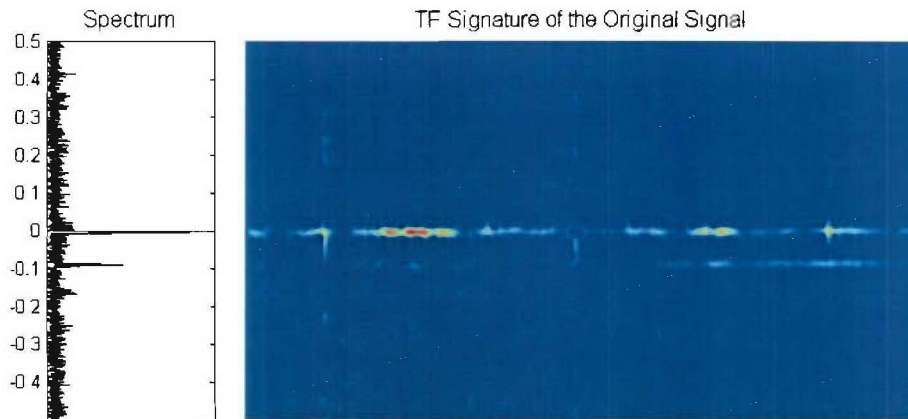


*Figure 28: Time-frequency signature of the original signal at range cell 124*
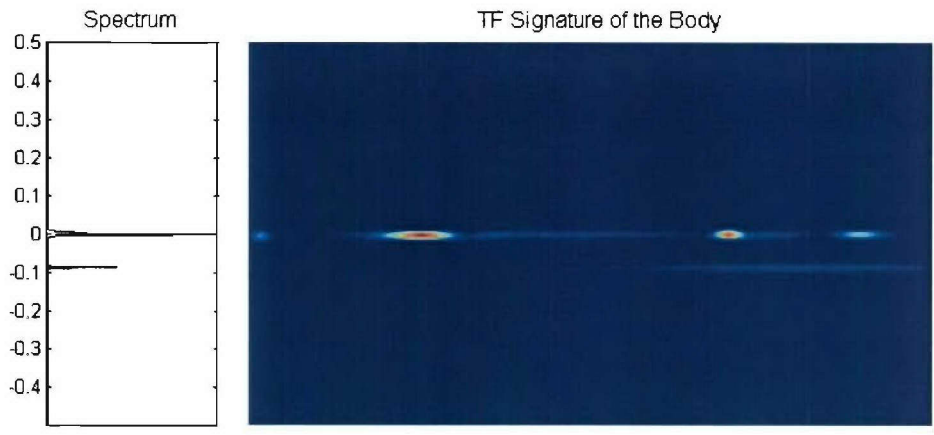
**Figure 29:** *Time-frequency signature of the extracted body signal at range cell 124*
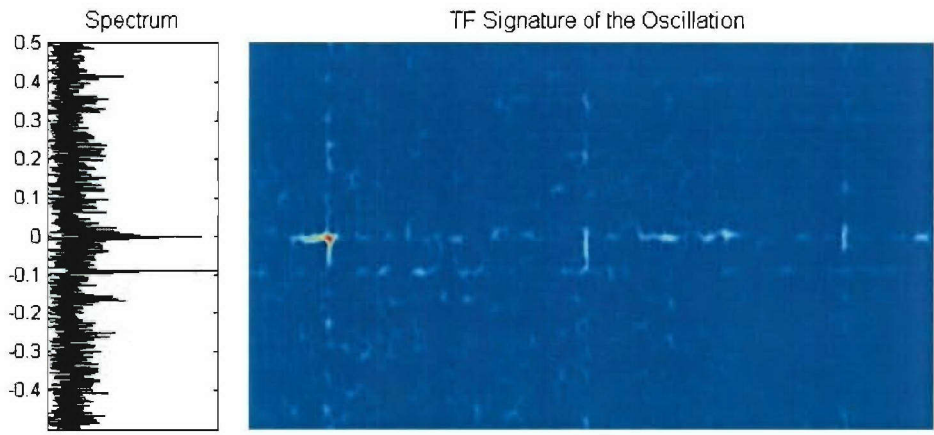


**Figure 30:** *Time-frequency signature of the extracted oscillating signal at range cell 124*
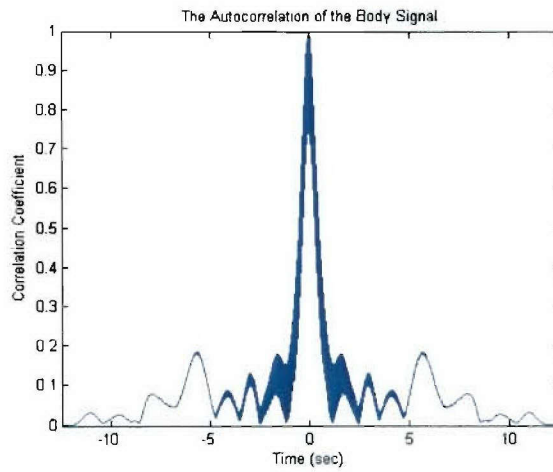
*Figure 31*: *Autocorrelation function versus time for the extracted body signal at range cell 124*
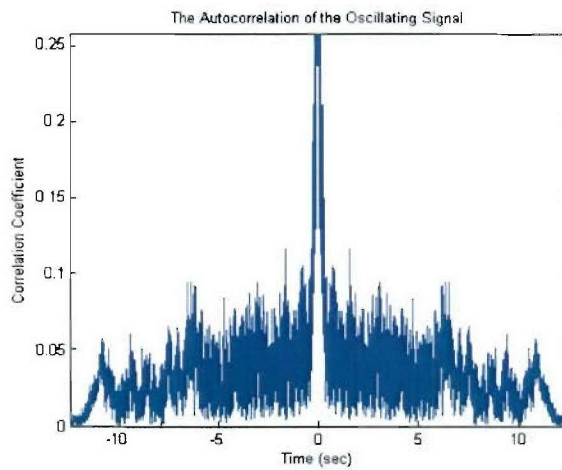


*Figure 32*: *Autocorrelation function versus time for the extracted oscillating signal at range cell 124*

# 4 Analysis Results

The results obtained from both the analysis using the wavelet decomposition method and the adaptive chirplet decomposition method allow the rotation rate of the antenna to be estimated. This is done by examining the time-series of the original data, the time-frequency signature of the extracted oscillating signal, and the autocorrelation of the extracted oscillating signal for each of the range cells (using both methods).

Using the time-frequency plot, the rotation rate of the antenna is estimated by measuring the time interval between peaks. The period is the time interval between peaks. As an example, in Figure 9, there are 3 peaks. The time interval between peak 1 and peak 2, between peak 2 and peak 3, and between peak 1 and peak 3 are measured. The average value is then used to estimate the rotation rate of the antenna. The period of the rotating antenna can be estimated by taking the autocorrelation of the time sequence. The peaks in correlation coefficient correspond to the dominant period of the signal.

The results of range cells 121 and 125 are not clear enough to provide any significant indications towards the rotational rate for either method. However, for the data analyzed herein, the rotational rate can be estimated for range cells 122, 123, and 124. These values are given in Table 2.

The actual antenna rotational rate is known to be 4.7 seconds. Clearly, the estimated values for both the wavelet decomposition method and the adaptive chirplet decomposition method for range cells 122, 123, and 124 correspond directly with the known value.

Overall, range cell 123 gives the best results for both methods. This is evident by looking at the time-frequency signatures of the original and extracted signals. Specifically, the oscillations of the rotating antenna can be clearly seen by looking at the time-frequency signatures of the extracted oscillating signal in Figures 9 and 23 (the wavelet and chirplet methods respectively). Furthermore, the autocorrelations of the extracted oscillating signal in Figures 11 and 25 (wavelet and chirplet

*Table 2: Estimated Rotation Rate of the Antenna (seconds)*

| Range Cell | Wavelet Decomposition | Adaptive Chirplet Decomposition |
|---|---|---|
| 122 | 4.6 | 4.4 |
| 123 | 4.8 | 4.8 |
| 124 | 4.7 | 4.8 |

respectively) both give the estimated rotation rate to be 4.8 seconds, which is very close to the actual value of 4.7 seconds.

# 5 Conclusion

Moving targets cause phase modulation of the SAR phase history corresponding to the target. A special case is rotating point targets. This report examines the case of a rotating antenna within in a SAR target scene collected by the US Navy APY-6 radar. Rotating target causes sinusoidal phase modulation of the azimuth phase history of the SAR collection. The phase modulation may equivalently be seen as a time-varying Doppler frequency. Time-frequency methods are useful tools in the analysis of such signals as they use time integration while still allowing for non-stationary signals.

In this report, we present two approaches for m-D analysis for the extraction of the m-D features of radar returned signals from targets in a SAR scene. Both approaches have two main processes; the first being the decomposition of the SAR return in order to extract m-D features, and the second being the time- frequency analysis in order to estimate motion parameters of the target in the SAR image. Two different approaches are used in the decomposition process. The first approach, a wavelet decomposition analysis, has been used in our previous m-D analysis work for a ISAR system, and it is presented here for the extraction of m-D features for a SAR system. The second approach, an alternative to the wavelet approach, is a new approach that is introduced for decomposing the time domain radar signal in SAR based on the adaptive chirplet decomposition. Different time-frequency techniques are employed depending on the procedure used in the decomposition process. For the wavelet based approach, the short-time Fourier transform is utilized, while in the procedure based on the adaptive chirplet decomposition, the time-frequency distribution series is used.

By applying the proposed procedures to data from a rotating antenna, the effectiveness of both these analysis techniques in a SAR target scenarios is confirmed. From the extracted m-D signatures, information about the target's micro-motion dynamics, such as rotation rate, has been obtained.

As demonstrated, both wavelet-based and chirplet-based procedures are successful for the extraction of m-D features from SAR data. The wavelet based method requires the decomposed signal's constituent parts to be combined in a specific manner in order to extract m-D features. While this is not the case for the chirplet based method, the chirplet based method still requires its alpha and beta parameters to be specifically set in order to extract any m-D features. The chirplet based method establishes itself to be a viable alternative. In general, however, it is shown that the results are much improved after the m-D extraction from the SAR target scenarios has taken place since only the vibration/rotational components are employed. The rotating frequency of the antenna was calculated using these two approaches and the results agree well with available ground truth. Such motion parameters may be

useful for describing the target, or serve as inputs to automatic target recognition algorithms.

## Acknowledgments

# References

1. Oliver, C. and Quegan, S. (1998). Understanding synthetic aperture radar images, *Artech House,* Boston.

2. Fransceschetti, G. and Lanari, R. (1999). Synthetic aperture radar processing, *CRC press LLC,* Boca Raton.

3. Curlander, J. C. and McDonough, R. N. (1991). Synthetic aperture radar - system and signal processing, Wiley and Sons, New York.

4. Carrara, W. G., Goodman, R. S., and Majewski, R. M. (1995). Spotlight synthetic aperture radar - signal processing alogorithm, *Artech House,* Norwood, MA.

5. Wehner, D. (1995). High-resolution radar, *Artech House,* Norwood, MA.

6. Soumekh, M. (1999). Synthetic aperture radar signal processing with Matlab algorithms, *Wiley and Sons,* New York.

7. Chen, V.C. and Ling, H. (2002). Time-Frequency transform for radar imaging and signal analysis, *Artech House,* BOSTON.

8. Chen, V. C. (2000). Analysis of Radar Micro-Doppler Signature with Time Frequency Transform, *Proc. Tenth IEEE Workshop on Statistical Signal and Array Processing,* pp. 463-466.

9. Li, J., and Ling, H. (2003). Application of adaptive chirplet representation for ISAR feature extraction from targets with rotating parts, *IEE Proc-Radar Sonar Navig.,* Vol. 150, No. 4, pp. 284-291.

10. Sparr, T., and Krane, B. (2003). Micro-Doppler analysis of vibrating targets in SAR, *IEE Proc-Radar Sonar Navig.,* Vol. 150, No. 4, pp. 277-283.

11. Thayaparan, T. (2004). Micro-Doppler radar signatures for intelligent target recognition, *DRDC Ottawa TM 2004-170,* Defence R&D Canada - Ottawa.

12. Thayaparan, T. and Abrol, S., and Riseborough, E. (2004). Micro-Doppler feature extraction of experimental helicopter data using wavelet and time-frequency analysis, *Radar 2004,* October 19-22, Toulouse, France.

13. Thayaparan, T. and Abrol, Chen, V. C. (2004). Analysis of micro-Doppler radar signatures from experimental helicopter and human data, *NATO SET-080 symposium,* October 11-13, Oslo, Norway.

14. Greneker, G., Geisheimer, J., and Asbell, D., "Extraction of Micro-Doppler from Vehicle Target at X-band Frequency,' Proceeding of SPIE on Radar Technology, Vol. 4374, 2001.

15. Wellman, R.J., and Silvious, J. L. (1998). Doppler Signature Measurements of an Mi-24 Hind-D Helicopter at 92 GHz, ARL-TR-1637, *Army Research Laboratory,* Adelphi, Maryland.

16. Bell, M. R., and Grubbs, R. A. (1993). JEM Modeling and Measurement for Radar Target Identification, *IEEE Trans. Aerospace Electron. Syst.,* Vol. 29, pp.73-87.

17. Sommer, H. and Salerno, J. (1971). Radar Target Identification System, U.S. Patent 3, pp. 614,779.

18. van Dorp, P., and Groen, F. C. A. (2003). Human walking estimation with radar", *IEE Proc-Radar Sonar Navig.,* Vol. 150, No. 5.

19. Geisheimer, J. L., Greneker, E. F., and Marshall, W. S., A High-Resolution Doppler Model of Human Gait, Georgia Tech Research Institute, 7220 Richardson Rd., Smyrna, GA 30080.

20. Qian, S. (2002). Introduction to time-frequency and wavelet transforms, *Prentice Hall PTR,* New Jersey.

21. Sheng, Y. (1995). Wavelet Transform, in the book the transforms and applications handbook. A. D. Poulariskas Ed., Chap. 10, pp. 747-827. *CRC and IEEE Press,* Boca Raton.

22. Strang, G and Nguyen, T. Q. (1995). Wavelet and Filter Banks, *Wellesley-Cambridge Press,* Wellesley, Massachusetts.

23. Mallat, S. (1989). A theory for multiresolution signal decomposition: The wavelet representation, *IEEE Trans. Pattern Anal. Machine Intell.,* Vol. 11, pp. 674-693.

24. A.U.G. Signals Ltd. (2002). Time-frequency algorithms for focussing distorted ISAR images, Contract No. W7714-011498/001/SV.

25. Yin, Q., Qian, S., and Feng, A. (2002). A fast refinement for adaptive Gaussian chirplet decomposition, *IEEE Trans. Signal Process.,* 50, (6), pp. 1298-1306.

26. Chen, V. and Ling, H. (1999). Joint time-frequency analysis for radar signal and image processing, *IEEE Signal Processing Mag.,* Vol. 16, pp. 81-93.

27. Trintinala, L. C. and Ling, H. (1997). Joint time-frequency ISAR using adaptive processing, *IEEE Trans. Antennas Propagat.,* Vol. 45, pp. 221-227.

28. Wang, G., Xia, X.-G., Root, B. T., Chen, V. C., Zhang, Y., and Amin, M.(2003). Manoeuvring target detection in over-the-horizon radar using adaptive clutter rejection and adaptive chirplet transform, *IEE Proc-Radar Sonar Navig.*, Vol. 150, No. 4, pp. 292-298.

29. Qian, S., Dunham, M. E., and Freeman, M. J. (1995). Trans-ionospheric signal recognition by joint time-frequency representation, *Radio Science,* Vol. 30., No. 6, pp. 1817-1829.

30. Wang, J. and Zhou, J. (1999). Chirplet-based signal approximation for earthquake ground-motion model, *IEEE Signal Processing Mag.*, Vol. 16, pp. 94-99.

31. Bell, M. R., and Grubbs, R. A. (1993). JEM Modeling and Measurement for Radar Target Identification, *IEEE Trans. Aerospace Electron. Syst.*, Vol. 29, pp.73-87.

## DOCUMENT CONTROL DATA
(Security classification of title, body of abstract and indexing annotation must be entered when the overall document is classified)

| 1. ORIGINATOR (the name and address of the organization preparing the document. Organizations for whom the document was prepared, e.g. Establishment sponsoring a contractor's report, or tasking agency, are entered in section 8.)<br><br>Defence R&D Canada – Ottawa<br>Ottawa, Ontario, Canada K1A 0Z4 | 2. SECURITY CLASSIFICATION (overall security classification of the document, including special warning terms if applicable)<br><br>UNCLASSIFIED |
|---|---|

**3. TITLE** (the complete document title as indicated on the title page. Its classification should be indicated by the appropriate abbreviation (S,C or U) in parentheses after the title.)

    Micro-Doppler analysis of rotating target in SAR (U)

**4. AUTHORS** (Last name, first name, middle initial)

    Thayaparan, Thayananthan; Abrol, Sumeet; Qian, Shie

| 5. DATE OF PUBLICATION (month and year of publication of document)<br><br>November 2005 | 6a. NO. OF PAGES (total containing information. Include Annexes, Appendices, etc.)<br><br>43 | 6b. NO. OF REFS (total cited in document)<br><br>31 |
|---|---|---|

**7. DESCRIPTIVE NOTES** (the category of the document, e.g. technical report, technical note or memorandum. If appropriate, enter the type of report, e.g. interim, progress, summary, annual or final. Give the inclusive dates when a specific reporting period is covered.)

    DRDC Ottawa Technical Memorandum

**8. SPONSORING ACTIVITY** (the name of the department project office or laboratory sponsoring the research and development. Include the address.)

    Defence R&D Canada – Ottawa
    Ottawa, Ontario, Canada K1A 0Z4

| 9a. PROJECT OR GRANT NO. (if appropriate, the applicable research and development project or grant number under which the document was written. Please specify whether project or grant)<br><br>13ec05 | 9b. CONTRACT NO. (if appropriate, the applicable number under which the document was written) |
|---|---|

| 10a. ORIGINATOR'S DOCUMENT NUMBER (the official document number by which the document is identified by the originating activity. This number must be unique to this document.)<br><br>DRDC Ottawa TM 2005-204 | 10b. OTHER DOCUMENT NOS. (Any other numbers which may be assigned this document either by the originator or by the sponsor) |
|---|---|

**11 DOCUMENT AVAILABILITY** (any limitations on further dissemination of the document, other than those imposed by security classification)

    ( X ) Unlimited distribution
    (  ) Distribution limited to defence departments and defence contractors; further distribution only as approved
    (  ) Distribution limited to defence departments and Canadian defence contractors; further distribution only as approved
    (  ) Distribution limited to government departments and agencies; further distribution only as approved
    (  ) Distribution limited to defence departments; further distribution only as approved
    (  ) Other (please specify):

**12. DOCUMENT ANNOUNCEMENT** (any limitation to the bibliographic announcement of this document. This will normally correspond to the Document Availability (11). However, where further distribution (beyond the audience specified in 11) is possible, a wider announcement audience may be selected.)

13. ABSTRACT ( a brief and factual summary of the document. It may also appear elsewhere in the body of the document itself. It is highly desirable that the abstract of classified documents be unclassified. Each paragraph of the abstract shall begin with an indication of the security classification of the information in the paragraph (unless the document itself is unclassified) represented as (S), (C), or (U). It is not necessary to include here abstracts in both official languages unless the text is bilingual).

(U) Rotating targets cause phase modulation of the azimuthal phase history of a SAR system. The phase modulation may be seen as a time-dependent micro-Doppler (m-D) frequency. Due to their superior resolution potential, it is useful to analyze such signals with time-frequency analysis methods. This report presents two approches for extracting m-D features from SAR images. In order to extract m-D features from SAR images, the time domain radar return is decomposed in two separate ways. One is based on wavelet decomposition in which the returned signal is decomposed into a set of components that are represented at different wavelet scales. The components are then reconstructed by applying the inverse wavelet transform. This wavelet approach has been used in our previous m-D analysis work for a ISAR system, and it is presented here in the extraction of m-D features for a SAR system. The second approach is based on adaptive chirplet decompostion. This new approach is introduced as an alternative to the wavelet approach of decomposing the SAR radar return. The results from the wavelet and adaptive chirplet decompostion procedures are compared, and the chirplet-based approach establishes itself as a viable alternative. The chirplet based method of m-D extraction has been successfully applied to SAR data scene collected by the US Navy APY-6 radar. The rotating frequency of the antenna was calculated using this method and the results agree well with available ground truth data.

14. KEYWORDS, DESCRIPTORS or IDENTIFIERS (technically meaningful terms or short phrases that characterize a document and could be helpful in cataloguing the document. They should be selected so that no security classification is required. Identifiers such as equipment model designation, trade name, military project code name, geographic location may also be included. If possible keywords should be selected from a published thesaurus. e.g. Thesaurus of Engineering and Scientific Terms (TEST) and that thesaurus-identified. If it is not possible to select indexing terms which are Unclassified, the classification of each should be indicated as with the title.)

SAR
ISAR
Wavelet
Time-Frequency Analysis
Chirplet Transform
Micro-Doppler
Target Detection
Fourier Transform
Doppler Processing
Phase Modulation
Autocorrelation

## Defence R&D Canada

Canada's Leader in Defence
and National Security
Science and Technology

## R & D pour la défense Canada

Chef de file au Canada en matière
de science et de technologie pour
la défense et la sécurité nationale

DEFENCE **R&D** DÉFENSE

www.drdc-rddc.gc.ca